TU/e EINDHOVEN UNIVERSITY OF TECHNOLOGY

Expanding thermal plasma CVD : experimental studies of the plasma-surface interaction

Citation for published version (APA):
Sanden, van de, M. C. M., Creatore, M., Blauw, M. A., Hoefnagels, J. P. M., Hoex, B., Oever, van den, P. J., Smets, A. H. M., Schram, D. C., & Kessels, W. M. M. (2005). Expanding thermal plasma CVD : experimental studies of the plasma-surface interaction. In A. Devi (Ed.), *EUROCVD-15 : Fifteenth European Conference on Chemical Vapor Deposition; proceedings of the international symposium; [held from 5th to 9th September 2005 in Bochum, Germany]* (pp. 36-48). (Proceedings - Electrochemical Society; Vol. 2005-09). Electrochemical Society, Inc..

Document status and date:
Published: 01/01/2005

Document Version:
Publisher's PDF, also known as Version of Record (includes final page, issue and volume numbers)

Please check the document version of this publication:

• A submitted manuscript is the version of the article upon submission and before peer-review. There can be important differences between the submitted version and the official published version of record. People interested in the research are advised to contact the author for the final version of the publication, or visit the DOI to the publisher's website.
• The final author version and the galley proof are versions of the publication after peer review.
• The final published version features the final layout of the paper including the volume, issue and page numbers.

Link to publication

General rights
Copyright and moral rights for the publications made accessible in the public portal are retained by the authors and/or other copyright owners and it is a condition of accessing publications that users recognise and abide by the legal requirements associated with these rights.

• Users may download and print one copy of any publication from the public portal for the purpose of private study or research.
• You may not further distribute the material or use it for any profit-making activity or commercial gain
• You may freely distribute the URL identifying the publication in the public portal.

If the publication is distributed under the terms of Article 25fa of the Dutch Copyright Act, indicated by the "Taverne" license above, please follow below link for the End User Agreement:

www.tue.nl/taverne

Take down policy
If you believe that this document breaches copyright please contact us at:

openaccess@tue.nl

providing details and we will investigate your claim.

Download date: 06. Nov. 2024

EXPANDING THERMAL PLASMA CVD: EXPERIMENTAL STUDIES OF THE PLASMA-SURFACE INTERACTION

M.C.M. van de Sanden, M. Creatore, M.A. Blauw, J.P.M. Hoefnagels, B. Hoex, P.J. van den Oever, A.H.M. Smets, D.C. Schram and W.M.M. Kessels
Department of Applied Physics, Equilibrium and Transport in Plasmas, Eindhoven University of Technology, P.O.Box 513, 5600 MB Eindhoven, The Netherlands
m.c.m.v.d.sanden@tue.nl

ABSTRACT

Fundamental studies which are relevant for the successful industrial implementation of the expanding thermal plasma set up, a novel plasma source characterized by high deposition rates (1-100 nm/s), are discussed. The plasma chemistry in Ar/O_2/hexamethyldisiloxane and Ar/O_2/octamethylcyclosiloxane-fed expanding thermal plasma setup and the influence of an additional ion bombardment during high rate silicon nitride deposition from $Ar/N_2/SiH_4$ and $Ar/NH_3/SiH_4$ mixture is reviewed. It is shown that the versatile control of parameters in the ETP setup (i.e., arc current, gas flow rates and working pressure) enable specific tuning of the film properties (i.e., chemical composition, optical and mechanical properties). In addition an example of a fundamental study of the gas phase and surface loss rates of Si and SiH_3 radicals during plasma deposition of hydrogenated amorphous silicon as obtained from time-resolved cavity ringdown absorption measurements are demonstrated.

Keywords: Expanding thermal plasma CVD, cratch resistant coatings, anti-reflection coatings, surface reaction probability, time-resolved cavity ringdown absorption

INTRODUCTION

Plasma deposition of thin films has specific advantages over other physical or chemical vapor deposition techniques because the dissociation of deposition precursors takes place in the gas phase, enabling the deposition of thin films on relatively cold substrates. Furthermore, the additional presence of ion bombardment, due to the difference in electron and ion mobility, enables the formation of high quality films since the surface mobility of deposition precursors can be enlarged and thus the surface and bulk morphology controlled. Usually plasma deposition also leads to higher deposition rates than physical and chemical vapor deposition techniques. These relative advantages have made plasma deposition the first choice in high value added industries such as e.g. the semiconductor industry. However, the deposition rates are usually rather low (< 1 nm/s), hampering the application of plasma deposition in large scale low added value applications such as barrier coatings on polymer substrates, thin film solar cells or scratch resistant coatings on polymer glazing. A fast plasma deposition technology which enables the deposition of high quality dense coatings would open up new markets for the application of plasma deposition technology. An example of a successful industrial implementation of a fast plasma deposition technique is the expanding thermal plasma (ETP) deposition technology as developed at the Eindhoven University of Technology. In this paper we will discuss shortly these successful implementations for the high rate deposition of scratch resistant $SiO_xC_yH_z$ coatings on

polymer substrates and a-SiN_x:H as anti-reflective coatings on multi-crystalline solar cells. These are only two examples of the films deposited using the ETP deposition technology. Other successful classes of thin films deposited at high rate using the ETP technology are a-Si:H [1], a-C:H [2] and ZnO [3]. An important aspect of the successful implementation is the fact that the scaling up of a plasma deposition technique requires a detailed knowledge of the deposition mechanism, which involves a detailed understanding of the surface processes as well as the gas phase chemistry. Some of these fundamental studies we have undertaken to unravel these complex processes will also be shortly discussed in this paper.

EXPANDING THERMAL PLASMA CVD

The expanding thermal plasma (ETP) technique, invented in our group almost two decades ago, combines a high-pressure plasma source with a low-pressure processing (deposition) reactor [4] (see Fig. 1a). The plasma source is a cascaded arc in which a plasma is generated by the application of a dc voltage to typically three cathodes that arc to one common grounded anode through a non-depositing carrier gas flowing through a narrow channel (see Fig. 1b). This carrier gas is often Ar but also H_2, N_2 or mixtures of these gases can be used. Due to the narrow channel, high gas flows and the plasma itself, the pressure in the plasma source is sub-atmospheric (typically 400 mbar) which means that the plasma is thermal. The electron and ion density in the channel is about 10^{15} cm^{-3} and due to the local thermal equilibrium the electron, ion, and gas temperature is equal and about 1 eV. The plasma expands through a nozzle into the low-pressure reactor and due to the pressure difference the expansion is first supersonic, and, after a stationary shock front (typically at ~5 cm from the nozzle at 0.2 mbar background pressure), subsonic. Due to the expansion behaviour, the electron temperature as well as the electron and ion density is sig-

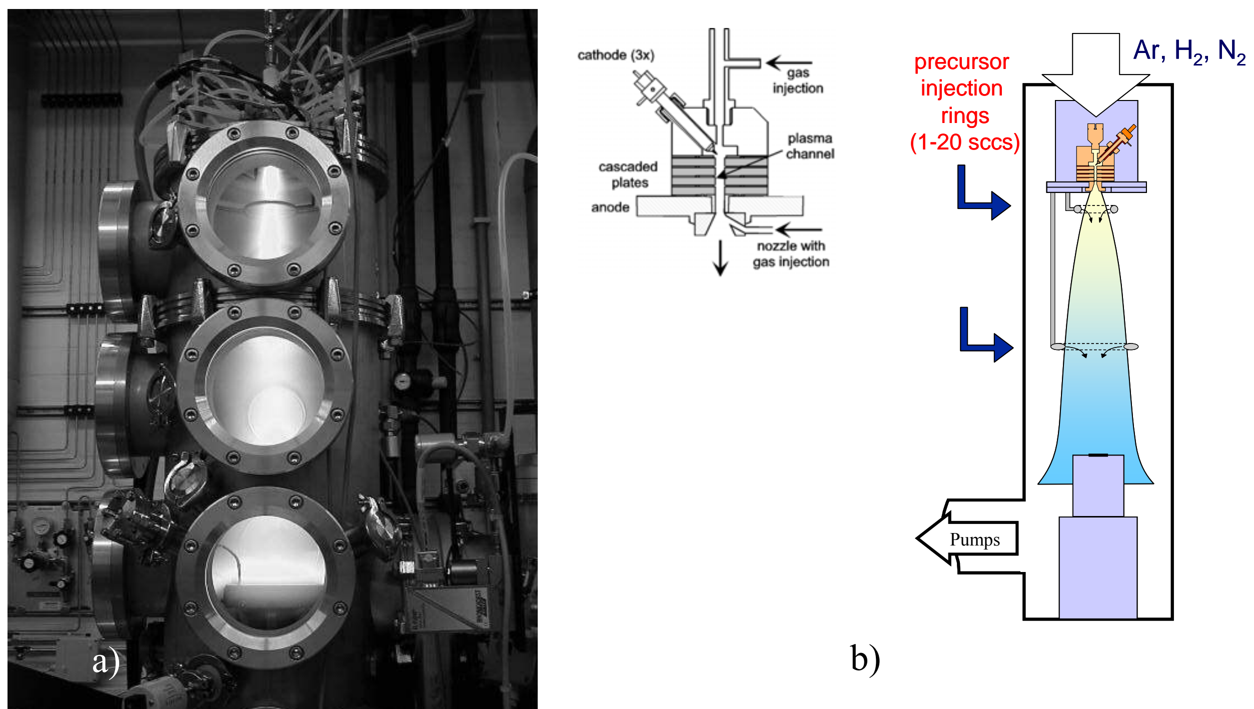

Figure 1 a) Expanding Thermal Plasma (ETP) set up and b) schematic of the ETP plasma source (i.e. cascaded arc + expansion zone).

nificantly reduced in the downstream region. The downstream electron temperature is typically 0.1-0.3 eV depending on the gases used and therefore electron-induced dissociation and ionization reactions can be neglected in the downstream region different from conventional plasma techniques. The downstream ion density on the other hand is relatively high (10^{13} cm^{-3} for pure Ar down to 10^{11} cm^{-3} for molecular plasmas) compared to other plasma techniques and this can be attributed to the fact that plasma creation takes place in a source at high pressure with consequently a much higher ionization degree than for low-pressure plasmas. Furthermore, when molecular gases such as H_2 and N_2 are admixed in the source, the frequent electron collisions and the high gas temperature cause also a high dissociation degree of the gases. This leads therefore also to large fluxes of H and N atoms from the source and, due to very effective dissociative ion-electron recombination reactions in the expansion zone for molecular gases, the plasma source operates under these conditions predominantly as an atomic H or N source (with the atom density typically a factor 10 – 100 higher than the ion density). Consequently, the high-pressure plasma source delivers very large flows of ions (Ar^+) or atoms (H, N) to the downstream region and therefore a large amount of "reactivity" to precursor gases such as e.g. NH_3 and SiH_4 that are injected downstream in the reactor. Due to the low electron temperature, these precursor gases are dissociated by ionic and/or atomic reactive species and due to the large amount of "reactivity" also much larger flows of precursor gases (the flows are typically in the order of 1 standard liter per minute (slm)) can be dissociated than in conventional low-pressure plasmas [1]. Two other important advantages of the ETP technique are that a relatively selective chemistry (e.g., precursor gas dissociation by Ar^+ or H by the selection of the carrier gas) can be chosen in contrast to electron-collision dominated plasmas and the fact that the source operation is not influenced at all by the downstream region (i.e., the ETP is the ultimate "remote plasma"). The latter aspect enables independent optimization of the upstream and downstream plasma region. The low pressure in the downstream region (generally 0.2 mbar, similar to typical pressures in rf parallel plate reactors) prevents excessive gas phase polymerization reactions and therefore abundant dust formation. Furthermore, the low electron temperature leads to very low substrate self-bias voltages, although additional rf substrate biasing can be applied to generate a controllable level of ion bombardment.
Within the last decade the ETP technique has been applied for the deposition of thin films of all kind of materials such as carbon [2] and silicon [1] films (amorphous, nanocrystalline, and diamond-like), oxides (silicon oxide [5] and zinc oxide [3]), and nitrides (carbon nitride and silicon nitride [6]). In all cases the deposition rates obtained were about an order of magnitude higher, i.e. well above other conventional (plasma enhanced) CVD methods, while maintaining film quality. Moreover, in recent years several companies have licensed the ETP technology for particular applications with as the two most important players General Electric [7] and OTB Engineering B.V.

ETP-CVD of scratch resistant $SiO_xC_yH_z$ coatings on polymer substrates: plasma and film studies.

Recently, an interest has arisen in the transportation and architectural industry to replace glass by polymeric materials. [7] Polymeric materials (e.g., polycarbonate) are equally transparent compared to glass but have the advantage of being light, flexible and rugged at the same time. However, in order to bypass the disadvantages of polymeric materials, i.e., UV-sensitivity and scratch-sensitivity, protective films are needed. In this contribution, the scratch-resistant film is addressed. Such a film will modify surface properties of the polymer, in particular it's tendency to be scratched, to ensure that the coated polymer is comparable to glass. For polycarbonate, the hardness/Young's modulus is typically 0.2/4 GPa whereas for glass these values are 5/75 GPa. Silicone ($SiC_xH_yO_z$) hard-coats have previously been applied to polycarbonate to accomplish

increased scratch-resistance using atmospheric wet coating technologies. Recently, alternative deposition techniques, such as chemical vapour deposition and plasma enhanced chemical vapour deposition (PECVD) have been developed for industrial applications because of their non-solvent approach and good adhesion of the films to the polymeric substrate. In particular, a novel organosilicon-based PECVD technique based on an Ar/O_2/hexamethyldisiloxane (HMDSO) and Ar/O_2/octamethylcyclotetrasiloxane (D4) expanding thermal plasma (ETP) source. Specifically, this technique enables the fast deposition of active organosilicon species from the plasma gas phase onto the polymeric surface. Due to the versatile control parameters of the setup and the chemical/physical character of the PECVD technique, the properties of the silicone films (e.g., chemical composition, optical and mechanical properties) can be tuned to the specific applications at hand, as will be shown further on [5,7]. At General Electric Global Research Center, the ETP source is already being employed in an industrial fast, large-area (multi-source) deposition reactor for silicone films on polycarbonate (GE Lexan® MR 10).
O_2 is injected into the plasma through the nozzle and HMDSO and D4 are injected through a ring located at approximately 5 cm from the outlet of the arc. Due to the low electron temperature, electron-monomer dissociation pathways are unlikely and the dissociation of HMDSO is controlled by dissociative recombination pathways involving Ar^+ and low energy electrons. The reactions in Eq. (1) show the possible dissociation of HMDSO molecules in the expanding thermal plasma [5]: a charge exchange occurs between the Ar^+ and the HMDSO molecule and subsequently, the HMDSO molecule can dissociate (dissociative recombination) at the Si-O, Si-C or C-H (Me = methyl group).

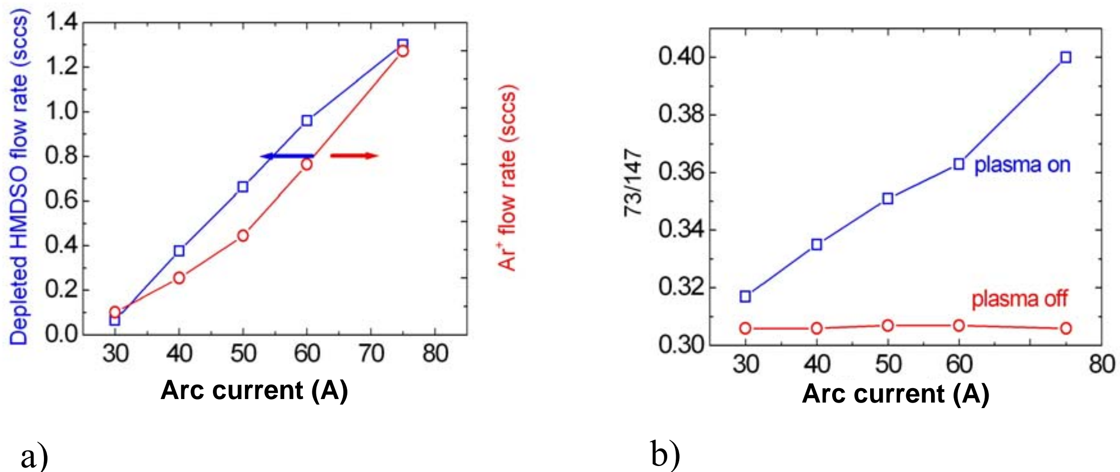

Figure 2 a) Mass spectrometry results of the depletion of the HMDSO molecule in comparison to the Ar^+ flow rate from the arc as a function of the arc current. b) 73 amu intensity normalised to the HMDSO parent ion (147 amu) intensity as a function of the arc current, when the plasma is turned on and off. Other experimental conditions: Φ_{Ar}=25 sccs, I_{arc}=50 A, Φ_{HMDSO}=2 sccs, $p_{reactor}$ =0.11 mbar.

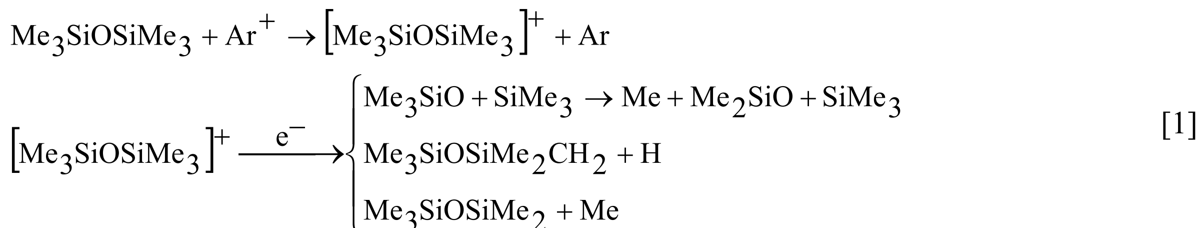

$$\mathrm{Me_3SiOSiMe_3 + Ar^+ \rightarrow [Me_3SiOSiMe_3]^+ + Ar}$$

$$\mathrm{[Me_3SiOSiMe_3]^+ \xrightarrow{e^-} \begin{cases} Me_3SiO + SiMe_3 \rightarrow Me + Me_2SiO + SiMe_3 \\ Me_3SiOSiMe_2CH_2 + H \\ Me_3SiOSiMe_2 + Me \end{cases}} \qquad [1]$$

Mass spectrometry measurements are performed to determine which of the reactions in Eqs. (1) occur in the ETP setup. Figure 2a. shows the depletion of the HMDSO molecule as a function of the arc current. In the same figure the Ar^+ flow rate, determined from Langmuir probe measurements [8], is also shown. It appears that the depletion of HMDSO molecule depends on the availability of Ar^+, which supports the charge exchange reaction in Eq. (1). In Fig.1b. the ratio of the fragment $Si(CH_3)_3^+$ (m/e=73 amu) and HMDSO (m/e=147 amu) intensities is shown as a function of the arc current, when the plasma is turned on and off. The fragment $Si(CH_3)_3^+$ is the parent ion of either the molecule $Si(CH_3)_4$ or the radical $Si(CH_3)_3$. A clear enhancement of the fragment is seen, when the plasma is turned on, indicating that $Si(CH_3)_3^+$ is created in the plasma phase. Being the only fragment for which this enhancement is seen, it is suggested that the Si-O bond of the HMDSO molecule is broken preferably in the ETP setup (second reaction in Eq. (1)) at least in conditions for which $[Ar^+] \cong [HMDSO]$. However, the breakage of the Si-O bond in the gas phase is not desirable as it represents the "mechanically strong" backbone for the deposition of scratch-resistant $SiC_xH_yO_z$ films. On the basis of the results mentioned above, in order to 'rebuild' the strong SiOSi network, it is necessary to dilute the HMDSO in O_2. The saturation of the depletion of O_2 depends on the limited availibility of Ar^+. However, at this point we cannot exclude reactions of molecular oxygen with HMDSO fragments. Second, the film characteristics have been analysed by means of spectroscopic ellipsometry. In Fig. 3a. the refractive index and the deposition rate of the film are shown as a function of the O_2 dilution. The increase of the deposition rate implies that O_2 affects the film growth, e.g. by reacting with HMDSO fragments. The details of the underlying mechanism will be studied in future work. The decrease of the refractive index to a value lower than the refractive index of SiO_2 ($\approx$1.46) implies that O_2 oxidises carbon (film etching) and creates voids. In Fig. 3b. the decrease of the imaginary part of the dielectric function at low wavelengths indicates a decrease in UV absorption by the film, which in turn is caused by carbon incorporated in the film.
In order to realize a capable large area high-rate coating process, a reactor in which two ETP sources were carefully spaced at a distance corresponding to the effective width of the single-ETP process profile [7]. In addition, injection rings that would insure uniform gas injection around the two ETP sources were designed, constructed, and installed onto the dual-ETP source

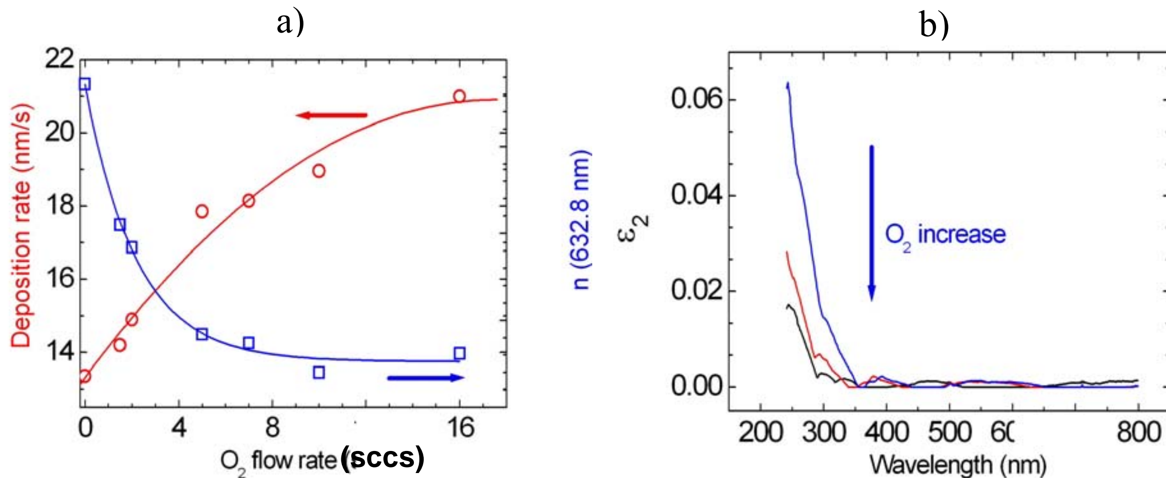

Figure 3 a) Spectroscopic ellipsometry results of the deposition rate and refractive index of the deposited films as a function of the O_2 flow rate in the gas phase. b) Spectroscopic ellipsometry results of the imaginary part of the dielectric function as a function of the O_2 flow rate in the gas phase. Other experimental conditions: Φ_{Ar}=25 sccs, I_{arc}=50 A, Φ_{HMDSO}=2 sccs, $p_{reactor}$=0.11-0.16 mbar.

reactor. Deposition experiments in which $SiO_xC_yH_z$ coatings, which can serve as abrasion resistant coatings, are deposited from a mixture of D4 and oxygen on 45 cm × 45 cm polycarbonate substrates that were pre-coated with a silicone hardcoat (GE Lexan® MR10) were performed. The mixtures of D4 and oxygen were injected through a single injection ring that surrounds both ETP sources. Prior to deposition, the substrates were preheated to temperatures around 100 °C. The substrates were translated in a single pass by the dual-ETP source array at a speed of 2.5 cm/s. The inner 30 cm × 30 cm area of the coated substrates, which had a coating thickness non-uniformity of less than 5% sigma/mean, were evaluated for abrasion resistance using the Taber abrasion method (ASTM D1044-94), i.e., the increase in haze was measured after ~1000 cycles of Taber abrasion using CS10F wheels with a 500 g load were performed.

ETP-CVD of anti-reflection coatings on multi-crystalline solar cells: rf/lf bias and film studies.

Silicon nitride films have been deposited by the ETP using the reactant mixtures N_2-SiH_4 and NH_3-SiH_4 [6]. When using the N_2-SiH_4 reactant mixture, an Ar-H_2-N_2 gas mixture is injected in the cascaded arc at a typically flow ratio of 3.3 slm : 0.3 slm : 0.6 slm and an arc current of 45 A. SiH_4 is injected in the downstream expansion zone by means of an injection ring at a typical flow up to 1 slm (1 slm is equivalent to 1000 sccm or about 16.7 sccs). For the NH_3-SiH_4 reactant mixture, the cascaded arc is operated on pure Ar while NH_3 is injected in the plasma through the nozzle (see Fig. 1b) and SiH_4 through the injection ring. The Ar and NH_3 flows are typically 3.3 slm and 1 slm respectively while the SiH_4 flow is typically varied between 0.05 and 0.3 slm. The arc current is within the range 45-75 A. For both types of plasmas, the downstream pressure is approximately 0.20 mbar. To study the material properties, the a-SiN_x:H films are deposited on different types of substrates (c-Si, mc-Si wafers) with a maximum size of 10 ×10 cm^2. The substrate temperature is actively controlled and is typically 400 ºC [6].
With both types of plasmas, a-SiN_x:H films can be deposited at very high deposition rates, i.e., up to 20 nm/s. However, in our experiments the films are typically deposited at a rate of ~5 nm/s [6]. A very important aspect of plasma deposition is that the refractive index of the a-SiN_x:H films can be accurately tuned by varying the SiH_4/N_2 or SiH_4/NH_3 flow ratio as a good control of the refractive index is necessary to optimize the antireflection coating (ARC) performance of the a-SiN_x:H film. Depending on the solar cell and panel design, a refractive index of ~2.0 (at 2 eV) gives the best ARC performance in air while a refractive index of ~2.4 (at 2 eV) gives the best ARC performance behind glass [9,10]. As shown in Fig. 4, the refractive index can be precisely tuned by operating the ETP at different flow mixtures. However, another requirement is that the absorption losses in the a-SiN_x:H are kept sufficiently low. When the refractive index is raised, the extinction coefficient of the a-SiN_x:H increases as also shown in the Fig. 4. The aim is therefore to obtain a-SiN_x:H films with a refractive index between 2.0-2.4 (at 2 eV) while keeping the extinction coefficient as low as possible. Generally the extinction coefficient at 3.44 eV is considered as for higher photon energies the transmission through the solar cell encapsulation material (glass with ethylene-vinyl acetate (EVA) foil) drops to zero [10]. This goal can be reached by the deposition of relatively N-rich films (to obtain low absorption) at a relatively high atomic film density (to obtain a sufficiently high refractive index). Furthermore, the film density and refractive index play also important role in obtaining the required degree of bulk passivation as will be discussed below.
A possibility to obtain a high film density at relatively low substrate temperatures is the application of external substrate biasing. Due to the low electron temperature in the ETP plasma the self-bias at the substrate is very low and therefore there is no significant ion bombardment of the substrate. A controllable level of ion bombardment can however be obtained by the applicati-

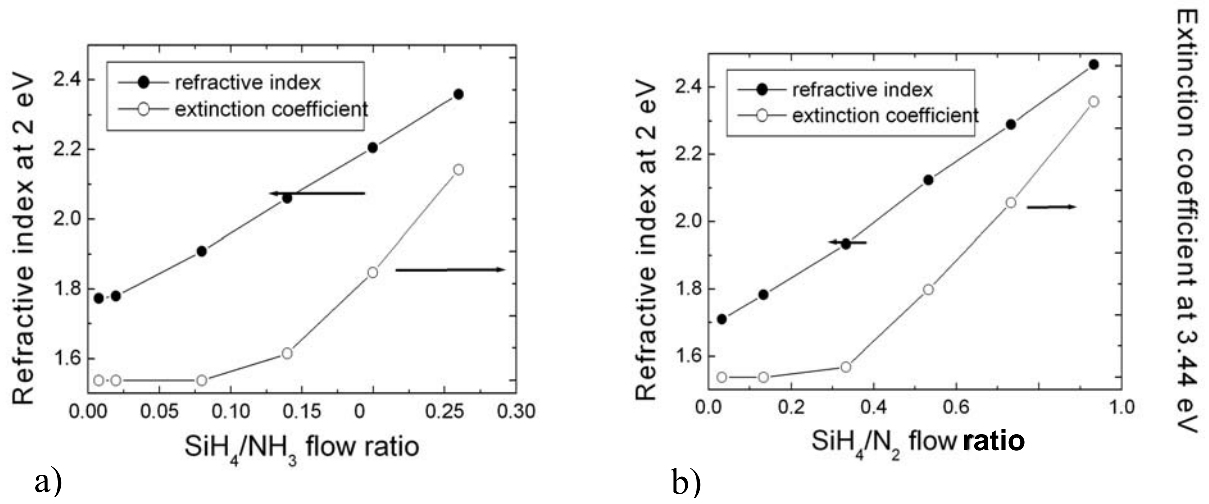

Figure 4 Refractive index (at 2 eV) and extinction coefficient (at 3.44 eV) for different flow ratios of (a) SiH_4 and NH_3 and (b) SiH_4 and N_2.

on of lf or rf power to the substrate. This external substrate biasing has been explored in an industrial type of ETP reactor for a-SiN_x:H films deposited from an Ar-NH_3-SiH_4 plasma at substrate temperatures <150 ºC using different starting conditions for the rf and lf case [11]. As reported in [11], the increase in film density with increasing dc bias voltage is up to 20%. This increase can for a large part be attributed to additional N incorporation into the film while no influence of the dc bias on the deposition rate has been observed [11].

As mentioned above, an a-SiN_x:H anti-reflection coating does not only reduce the optical losses but it can also provide surface and bulk passivation of the solar cells. For solar cells of mc-Si with screen printed contacts and a highly doped emitter, surface passivation is not yet an important issue, however bulk passivation of the cells by the hydrogen released from the a-SiN_x:H layer can enhance the efficiency of the solar cells by ~15% (relative). This means that the efficiency of a typical mc-Si solar cell with an TiO_2 ARC can be increased from ~12.0-12.5 % to approximately 14% by the application of an a-SiN_x:H ARC. This efficiency can be raised further (to an efficiency over 15%) by using a lower doping level for the emitter and by applying surface texture for better light trapping, etc.

To study whether such an enhancement in efficiency can be achieved by an a-SiN_x:H ARC deposited at high-rate by the ETP technique, several lab-scale experiments have been carried out. First, it has been verified that a good ARC performance can be obtained by a-SiN_x:H films deposited from both the N_2-SiH_4 and NH_3-SiH_4 reactant mixture. As shown in figs. 4, the optical properties of the film are fully tunable by the plasma conditions and for mc-Si solar cells (with a size of 10×10 cm^2) it has been shown that the reflectivity can be minimized using ETP a-SiN_x:H (using both reactant mixtures) with the right combination of refractive index and film thickness [6]. The results by Hong et al. [6] are similar to those obtained by state-of-the-art a-SiN_x:H films deposited by a remote microwave (MW) plasma at a rate of <1 nm/s. The fact that the a-SiN_x:H deposited from the Ar-H_2-N_2-SiH_4 plasma acts as a good ARC has also been proven by the production of laboratory c-Si solar cells (with a size of 2×2 cm^2). Due to the a-SiN_x:H ARC, the efficiency of the optimized cells increased from 12.8% to 18.1%, mainly due to the increase in short-circuit current [see Kessels et al., 6]. This gain in efficiency is only slightly lower than the

reference cells coated with an rf parallel plate capacitively coupled plasma which also induce a high degree of surface passivation [6]. After establishing the ARC performance of the ETP deposited a-SiN_x:H, it has been tested whether the a-SiN_x:H films also induce bulk passivation. Therefore solar cells produced from mc-Si wafers from the adjacent positions in the ingot have been coated by a-SiN_x:H films using the two different reactant mixtures. Furthermore, reference cells have been produced using state-of-the-art a-SiN_x:H deposited from a remote MW NH_3-SiH_4 plasma and by producing "reverse scenario cells" [6]. The cells with a-SiN_x:H deposited from both the N_2-SiH_4 reactant mixture and NH_3-SiH_4 reactant mixture (see Fig. 8), showed an increase in the Internal Quantum Efficiency at near-infrared wavelengths compared to the reverse scenario cell [6]. This so-called enhanced "red-response" indicates that bulk passivation is achieved. For the a-SiN_x:H deposited from the NH_3-SiH_4 reactant mixture, the increase is almost as high as for the state-of-the-art MW plasma deposited a-SiN_x:H, while the N_2-SiH_4 reactant mixture leads to a lower degree of bulk passivation. This is therefore a proof-of-principle that demonstrates that bulk passivation can be obtained by a-SiN_x:H deposited by the ETP at high-rate and that the NH_3-SiH_4 reactant mixture is favored over the N_2-SiH_4 reactant mixture. Further optimization has taken place in an industrial-type reactor which yields good film uniformity. On the basis of the aforementioned results, the ETP technique has been implemented for the deposition of a-SiN_x:H antireflection coatings on c-Si solar cells by the Netherlands-based company OTB Engineering B.V. [12].

Time resolved CRDS: determination of the surface reaction probability

Hydrogenated amorphous (a-Si:H) and microcrystalline silicon (μc-Si:H) thin films have important applications in semi-conductor devices and solar cell fabrication. In particular, a-Si:H and μc-Si:H are used in thin film transistors (TFTs) and the next generation thin film solar cells. Over the last few years, μc-Si:H has gained a lot of interest, because it exhibits important advantages compared to a-Si:H. Hydrogenated microcrystalline silicon has a lower bandgap (1.1 eV) than a-Si:H (1.7 eV), which enables a better use of the solar spectrum in tandem solar cell configurations [12]. Furthermore, it shows less light induced degradation [13] and a higher electron mobility. Future industrial applications of a-Si:H and μc-Si:H require deposition processes with a high growth rate (> 1 nm/s) and high film quality. High growth rate deposition of a-Si:H and μc-Si:H films is possible with the expanding thermal plasma (ETP) deposition technique. In this section we will discuss an experiment which we have conducted in the past to unravel an important aspect of the growth mechanism of silicon thin films using plasmas: the surface reaction probability of silicon radicals. The expanding thermal plasma, due to its remote nature, is in this respect also an excellent source to perform these studies.
For basic understanding and modeling of plasma deposition processes, information on the density as well as the surface reactivity of the plasma species is essential. Often the surface reaction probability β of the species has been obtained indirectly [14] or under process conditions different from the actual plasma deposition process, *e.g.*, from a molecular beam scattering experiment [15] or by time-resolved density measurements in an afterglow plasma [16,17]. In recent work we employed time-resolved cavity ringdown spectroscopy (τ-CRDS). τ-CRDS is used to obtain β *during* plasma deposition: the highly sensitive cavity ring-down spectroscopy (CRDS) method [18] is used to map an increased radical density due to a pulsed rf bias to the substrate in addition to the continuously operated remote SiH_4 plasma. Although time-resolved CRDS has been employed previously to obtain gas phase loss rates of radicals [19,20], in this work the technique has been extended to measurements of the surface loss rates of the radicals [21,22]. This simultaneously yields information on the surface reaction probability β and the

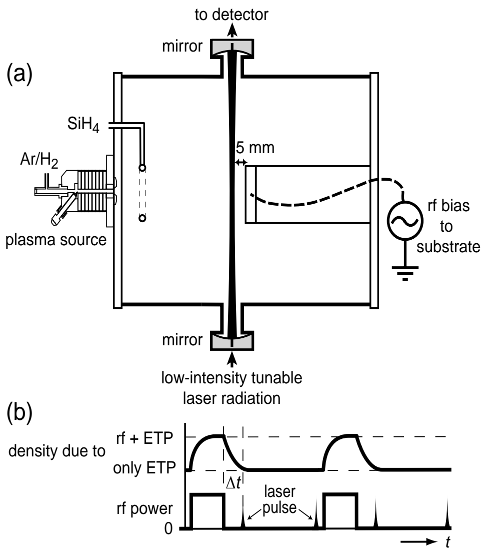

Figure 5 (a) The expanding thermal plasma (ETP) setup equipped with the cavity ringdown spectroscopic setup and an rf power supply for pulsed bias voltage application to the substrate. (b) Schematic time diagram illustrating the modulation of the radical density and the synchronization of the CRDS laser pulses.

density of the radicals under the specific plasma conditions, here particularly for the case of high rate deposition of hydrogenated amorphous silicon (a-Si:H) [23]. Using this method, it is shown that Si is mainly lost in the gas phase to SiH_4, whereas SiH_3 is only lost via diffusion to and reactions at the surface. Moreover, β of Si and SiH_3 are determined and it is shown that β_{SiH3} is independent of the substrate temperature.

In the expanding thermal plasma (ETP) technique [Fig. 5(a)] a remote expanding Ar-H_2-SiH_4 plasma is created. To detect (low-density) radicals such as SiH_3 and Si the CRDS technique has previously been employed; SiH_3 has been identified at the $\tilde{A}\,^2A_1{}' \leftarrow \tilde{X}\,^2A_1$ broadband transition ranging from ~200 to ~260 nm [24], whereas Si radicals have been probed at the 4s $^3P_{0,1,2} \leftarrow 3p^2\ ^3P_{0,1,2}$ transition around 251 nm [25]. In the time-resolved CRDS (τ-CRDS) measurements, a minor periodic modulation of the radical densities is produced by applying 5 Hz, 2.5% duty cycle rf pulses to the substrate in addition to the continuously operating ETP [22]. The additional absorption A_{rf} due to the radicals generated by the rf pulse is obtained from the difference in absorption at some point Δt in the rf afterglow and at a point long after the influence of the rf pulse has extinguished [see Fig. 5(b)]. Every CRDS trace is handled separately by means of a 'state-of-the-art' 100MHz, 12 bit data acquisition system [26] and an averaged A_{rf} is obtained as a function of time Δt in the afterglow of the rf pulse.

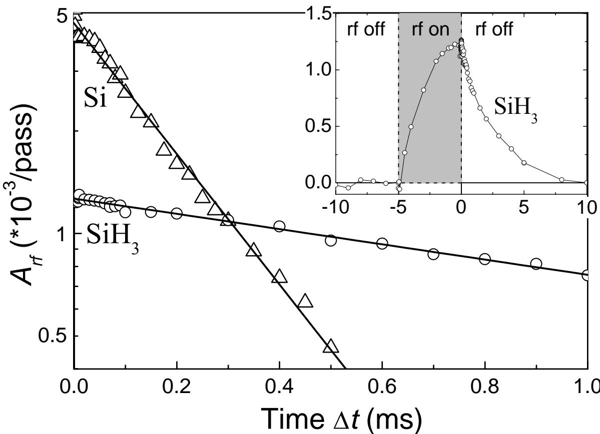

Figure 6 Typical semi-logaritmic plot of the additional absorption A_{rf} of Si and SiH_3 during the rf afterglow showing a single exponential decay with a loss time of (0.226±0.006) ms and (1.93±0.05) ms for Si and SiH_3, respectively. Every data point is an average of 128 CRDS traces. The inset shows a linear plot of the A_{rf} of SiH_3 for the complete rf pulse of 5 ms.

A typical τ-CRDS measurement for Si and SiH_3 is shown in Fig. 6. A duty cycle of 2.5 % has carefully been chosen in order to obtain a good signal-to-noise ratio in the additional Si and SiH_3 absorption, while possible powder formation due to the 'anion confining' rf plasma sheath is suppressed [27]. Fig. 6 shows that both Si and SiH_3 decrease single exponentially, which is expected from the radicals' mass balance [28]. The corresponding loss rate τ^{-1} depends linearly on the gas phase loss on one hand and the loss due to diffusion to and reactions at the surface on the other hand [26]:

$$\tau^{-1} = k_r n_x + \frac{D}{\Lambda^2} \qquad [2]$$

In this equation, k_r is the gas phase reaction rate with species x with density n_x, D is the diffusion coefficient for the specific radical in the Ar-H_2-SiH_4 mixture [29], and Λ is the effective diffusion length of the radical. The latter depends on diffusion geometry and on the radical's surface reaction probability β [28]. The gas temperature T_{gas} is necessary to calculate the density of SiH_4 via the ideal gas law, while T_{gas} is also needed to calculate the diffusion term in Eq. (2). Therefore, T_{gas} has been measured from the Doppler broadening of the Si 4s $^3P_2 \leftarrow 3p^2\,^3P_1$ atomic line. For all β measurements T_{gas}≈1500K and T_{gas} is independent of T_{sub} [28]. From Eq. (2) it is seen that the gas phase loss processes need to be considered first before surface loss rates of the radicals can be deduced. For Si and SiH_3 in the ETP plasma the only candidate for a significant gas phase loss is SiH_4 [29]. Therefore the loss rate of Si and SiH_3 has been obtained as a function of the SiH_4 density (Fig. 7) keeping the pressure and thus the diffusion term in Eq. (2) nearly constant. The SiH_4 density has been calculated from the SiH_4 partial pressure using T_{gas}=1500K including a correction for the local SiH_4 consumption [22]. The loss rate of SiH_3 in Fig. 7 is independent of the SiH_4 density, which indicates no gas phase loss of SiH_3, while the loss rate of Si increases linear with the SiH_4 density. The slope reveals a reaction rate constant of Si(^{3}P) with SiH_4 of k_r=(3.0±1.3)×10^{-16} $m^{-3}s^{-1}$. This value corresponds well with literature values [21,22].
To deduce the surface reaction probability β of Si and SiH_3 from Eq. (2), a semi-empirical expression with radial and axial diffusion length R and H, as proposed by Chantry [21,22,28], has been assumed for the cylinder symmetrical diffusion geometry of the ETP reactor. Then, for SiH_3

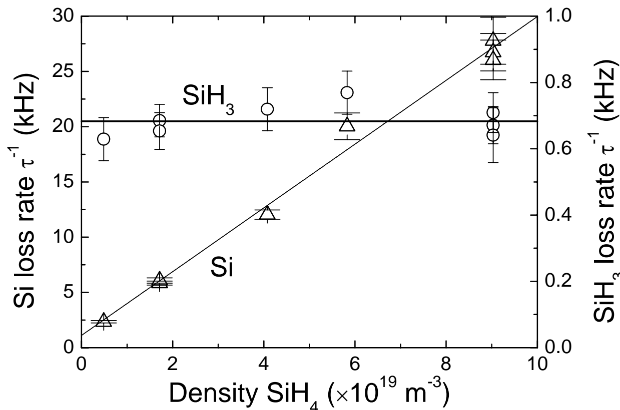

Figure 7 The loss rate of Si and SiH_3 as a function of the SiH_4 density keeping the total pressure constant at 0.27 mbar.

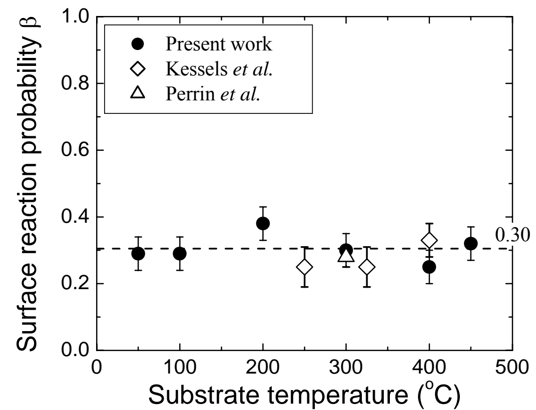

Figure 8 the surface reaction probability β o SiH_3 as deduced from the offsets of Fig. 6 a a function of T_{sub}. Also shown are values o β from literature, Refs. [14,16].

(no gas phase loss) the loss time τ in Eq. (2) depends linear on the pressure with a slope depending on R, H, and T_{gas} and an offset depending on R, H, T_{gas}, and β. After careful consideration it has been assumed that the diffusion of the radicals in radial direction can be neglected in respect to the diffusion in axial direction, i.e., $R \rightarrow \infty$ [21,22]. Subsequently, H can be obtained from the pressure dependence of the loss time of SiH_3. The obtained surface reaction probability β as a function of T_{sub} of the SiH_3 radical applying this procedure is shown in Fig. 8. No clear dependence of β_{SiH3} on T_{sub} is seen. The value obtained is in good agreement with estimated values of β_{SiH3} for 3 different T_{sub} as obtained previously with the indirect method of 'aperture-well assembly' applied under similar conditions in the same setup [14]. The value also corresponds to $\beta_{SiH3}=0.28\pm0.03$ at $T_{sub}=300$ °C as determined by Perrin *et al.* using time-resolved threshold ionization mass spectrometry in an rf plasma with a 100% on-off modulation [16]. For Si also the loss time has been measured as a function of the pressure. Assuming the same diffusion geometry for Si as for SiH_3, while taking into account the gas phase loss to SiH_4, a lower limit of 0.9 has been obtained for β of Si, yielding therefore $0.9<\beta_{Si}\leq1$. Although this is the first direct experimental evidence for a nearly unity surface reaction probability of Si, a β of ~1 is generally assumed for the Si radical on the basis of its hydrogen deficiency [17,28]. Based on (estimates of) the densities of all plasma species, combined with their β, it is found that SiH_3 has the main contribution to the a-Si:H film growth [11,28]. Furthermore, the independence of the β_{SiH3} on T_{sub} seems remarkable, because the surface structure depends strongly on T_{sub}. The implications of these observations and other observations on the growth mechanism of a-Si:H are discussed in [30].

CONCLUSIONS

In this paper we have discussed plasma chemistry and film modification studies relevant for two successful implementations of the novel ETP technology, scratch resistant films on polycarbonate substrates and anti-reflection and bulk passivation layers on multi-crystalline silicon solar cells. It has been shown that high quality thin films can be grown at high growth rate conditions (> 5 nm/s). Although not extensively addressed in this paper, much of the results have been enabled by the fundamental knowledge of the high rate deposition process, results which have been reported elsewhere, see for example Refs. [1-6,10,11,21-26,30].

ACKNOWLEDGEMENTS

The authors gratefully acknowledge A.J.M. van Erven, F.J.H. van Assche, J.H. van Helden, Y. Barrell, R. Vangheluwe, M.Evers, M. Bijker, M. Schaepkens, C.D. Iacovangelo, T. Miebach and Dr. R. Engeln for their contribution to the experiments. Parts of this study has been carried out within the E.E.T.-program "HR-CEL" and "Sunovation" funded by the Netherlands Ministry of Economic Affairs, the Ministry of Education, Culture and Science and the Ministry of Public Housing, Physical Planning and Environment. This research was furthermore supported by The Netherlands Foundation for Fundamental Research on Matter (FOM: 98PR1781 and 99PSI03). General Electric is thanked for their financial contribution to the Eindhoven research group. The research of W.K. has been made possible by a fellowship of the Royal Netherlands Academy of Arts and Sciences (KNAW). The authors acknowledge the Technical Laboratory Automation group of the Eindhoven University of Technology and the technical assistance by M.J.F. van de Sande, J.F.C. Jansen, H.M.M. de Jong, and A.B.M. Hüsken.

REFERENCES

1. M.C.M. van de Sanden, R.J. Severens, W.M.M. Kessels, R.F.G. Meulenbroeks, D.C. Schram, J. Appl. Phys **84**, 2426 (1998), W.M.M. Kessels, M.G.H. Boogaarts, J.P.M. Hoefnagels, D.C. Schram, M.C.M. van de Sanden, J. Vac. Sci. Technol. A 19, 1027 (2001)
2. J.W.A.M. Gielen, W.M.M. Kessels, M.C.M. van de Sanden, D.C. Schram, J. Appl. Phys. **82**, 2643 (1997), J.W.A.M. Gielen, M.C.M. van de Sanden, D.C. Schram, Appl. Phys. Lett. **69**, 152 (1996)
3. R. Groenen, J.L. Linden, H.R.M. van Lierop, D.C. Schram, A.D. Kuypers, M.C.M. van de Sanden, Appl. Surf. Sci. **173**, 40 (2001), R. Groenen, J. Löffler, P.M. Sommeling, J.L. Linden, E.A.G. Hamers, R.E.I. Schropp, M.C.M. van de Sanden, Thin Solid Films **392,** 226 (2001)
4. D. C. Schram and G. M. W. Kroesen, U.S. Patent No. 4,871,580 (1989); European Patent No. 0297637 (1992)
5. M. Creatore, M.F.A.M. van Hest, J.Benedikt, M.C.M. van de Sanden, MRS proc. **715**, 101 (2002), M.Creatore, M. Kilic, K. O'Brien, R.Groenen, M.C.M. van de Sanden, Thin Solid Films **427**, 137 (2003), M.F.A.M. van Hest, B. Mitu, D.C. Schram, M.C.M. van de Sanden, Thin Solid Films **449,** 52 (2004), Y. Barrell, M. Creatore, M. Schaepkens, C.D. Iacovangelo, T. Miebach, M.C.M. van de Sanden, Surf. Coat. Technol., **180-181** 367 (2004)
6. W.M.M. Kessels, J. Hong, F.J.H. van Assche, M.D. Moschner, T. Lauinger, W.J. Soppe, A.W. Weeber, D.C. Schram, and M.C.M. van de Sanden, J. Vac. Sci. Technol. A **20**, 1704 (2002), J. Hong, W.M.M. Kessels, W. J. Soppe, A.W. Weeber, W.M. Arnoldbik, and M.C.M. van de Sanden, J. Vac. Sci. Technol. B **21**, 2123 (2003), J. Hong, W.M.M. Kessels, F.J.H. van Assche, H.C. Rieffe, W.J. Soppe, A.W. Weeber, and M.C.M. van de Sanden, Prog. Photovolt: Res. Appl. **11**, 125 (2003)
7. M. Schaepkens, S. Selezneva, P. Moeleker, C.D. Iacovangelo, J. Vac. Sci. Technol. A 21, 1266 (2003), A. de Graaf, M.F.A.M. van Hest, M.C.M. van de Sanden, K.G.Y. Letourneur, D.C. Schram, Appl. Phys. Lett. **74**, 2927 (1999)
8. P. Doshi, G.E. Jellison, and A. Rohatgi, Appl. Opt. **36**, 7826 (1997)
9. H. Nagel, A.G. Aberle, and R. Hezel, Prog. Photovolt: Res. Appl. **7**, 245 (1999)
10. F.J.H. van Assche, W.M.M. Kessels, R. Vangheluwe, W.S. Mischke, M. Evers, and M.C.M. van de Sanden, accepted for publication in Thin Solid Films (2005)
11. M.C.M. van de Sanden, P. J. van de Oever, M. Creatore, M. Schaepkens, T. Miebach, C.D. Iacovangelo, R.C.M. Bosch, M. Bijker, M. Evers, D.C. Schram, W.M.M. Kessels, 47th Annual Technical Conference Society of Vacuum Coaters Proc., **447**, 2004.
12. J. Meier, S. Dubail, J. Cuperus, U. Kroll, R. Platz, P. Torres, J. A. A. Selvan, P. Pernet, N. Beck, N. P. Vaucher, et al., J. Non-Cryst. Solids **227-230**, 1250 (1998).
13. B. Rezek, J. Stuchlík, A. Fejfar, and J. Kočka, J. Appl. Phys. **92**, 587 (2002).
14. See e.g., W.M.M. Kessels, M.C.M. van de Sanden, R.J. Severens, and D.C. Schram, J. Appl. Phys. **87**, 3313 (2000) and references therein.
15. P.R McCurdy, K.H.A. Bogart, N.F. Dalleska, and E.R. Fisher, Rev. Sci. Instrum. **68**, 1684 (1997).
16. J. Perrin, M. Shiratani, P. Kae-Nune, H. Videlot, J. Jolly, and J. Guillon, J. Vac. Sci. Technol. A **16**, 278 (1998).
17. P. Kae-Nune, J. Perrin, J. Guillon, and J. Jolly, Plasma Sources Sci. Technol. **4**, 250 (1995).
18. K.W. Busch and M.A. Busch, Cavity-Ringdown Spectroscopy, Am. Chem. Soc., Wash. DC, (1999).
19. D.B. Atkinson and J.W. Hudgens, J. Phys. Chem. A, 101, 3901 (1997) and references therein.
20. A. P. Yalin, R. N. Zare, C. O. Laux, C. H. Kruger, Appl. Phys. Lett. **81**, 1409 (2002).

21. J.P.M. Hoefnagels, A.A.E. Stevens, M.G.H. Boogaarts, W.M.M. Kessels, and M.C.M. van de Sanden, Chem. Phys. Lett. **360**, 189 (2002).
22. J.P.M. Hoefnagels, Y. Barrell, M.C.M. van de Sanden, W.M.M Kessels, to be published.
23. W. M. M. Kessels, R. J. Severens, A. H. M. Smets, B. A. Korevaar, G. J. Adriaenssens, D. C. Schram, and M. C. M. van de Sanden, J. Appl. Phys. **89**, 2404 (2001).
24. W.M.M. Kessels, A. Leroux, M.G.H. Boogaarts, J.P.M. Hoefnagels, M.C.M. van de Sanden, and D.C. Schram, J. Vac. Sci. Technol. A. **19**, 467 (2001).
25. W.M.M. Kessels, J.P.M. Hoefnagels, M.G.H. Boogaarts, D.C. Schram, and M.C.M. van de Sanden, J. Appl. Phys. **89**, 2065 (2001).
26. Technical Laboratory Automation Group, Eindhoven University of Technology, Den Dolech 2, 5600 MB Eindhoven, The Netherlands.
27. C. Courteille, J.L. Dorier, C. Hollenstein, L. Sansonnens, and A.A. Howling, Plasma Sources Sci. Technol. **5**, 210 (1996).
28. P.J. Chantry, J. Appl. Phys. **62**, 1141 (1987).
29. J. Perrin, O. Leroy, and M.C. Bordage, Contrib. Plasma. Phys. **36**, 1 (1996).
30. W.M.M. Kessels, J.P.M. Hoefnagels, P.J. van de Oever, Y. Barrell, M.C.M. van de Sanden, Surf. Science **547**, L865-L870 (2003)